

Erosion and Sedimentation Modeling Using Delft3D in the Manikin Estuary, Kupang, East Nusa Tenggara

Alexandro T. Kolo^{a*}, A.A.N. Satria D. Negara^a

Correspondence

^aCivil Engineering Department,
Sepuluh Nopember Institute of
Technology , ITS Campus,
Surabaya 60111, Indonesia.

Corresponding author email address:
alexandrokolo@gmail.com

Submitted : 21 November 2025
Revised : 25 November 2025
Accepted : 28 November 2025

Abstract

The sedimentation and erosion of Manikin Estuary is analysed using numerical model DELFT3D. The model simulates the influence of river flow and coastal wave to induce the transport of sediment. The river flow is obtained from automatic water level data and suspended sediment is measured on site. The wave is hindcasted using spectral wave model SWAN with forcing from ERA 5 Reanalysis Data. The model is calibrated by comparing the coastline change from the model and satellite imagery. The simulation scenarios consider the combination of river discharge and waves condition in east season and west season. The simulation shows in the west season the dominant influence from high waves produces considerable erosion and sedimentation in the estuary and coastal areas, while high river discharge during the wet season has more influence on sedimentation and erosion in the river. Meanwhile, in the east season, the dominant influence from waves results in sedimentation and erosion that predominantly occurs in coastal areas even though the waves are relatively lower than the west season.

Keywords

Erosion, Sedimentation, Delft3D, Estuary, Coastline

INTRODUCTION

The river estuary as the downstream part of the river that is directly adjacent to the sea is a place of discharge accumulation from the river and the tidal processes. According to its function, the shape of the estuary must fulfill the function of a series of hydrodynamic processes in the coastal area. [1,2]. In addition, estuaries provide many benefits for communities and coastal ecosystems. Problems in the estuary area are one of the challenges in efforts to manage and utilize the estuary in supporting coastal ecosystems [3]. Sedimentation-erosion is one of the problems that have a major influence on estuarine and coastal ecosystems. Solid particle movement or sediment transport is a complex problem of bedform formation and migration that can affect circulation and water quality[4,5]. The hydrodynamic cycle and sediment transport of estuaries and coasts are influenced by waves, tides, and river discharge [6,7].

Sediment transport and erosion are critical natural processes that affect the dynamic activities of coastal areas and estuaries [8]. Such is the case of the Manikin coastal area, Kupang, East Nusa Tenggara. The Manikin Estuary and Beach area, located in the southwest of Timor Island in the semi-enclosed Kupang Bay region, has unique estuary morphological characteristics. The dynamics of river flows carrying sediments from upstream to downstream, as well as wave conditions and currents influenced by the west and east seasons are quite complex coastal hydrodynamics

cycles that show indications of shoreline changes, and erosion and sedimentation at the mouth of the estuary that cause siltation. Sediment deposition and shoreline changes due to accretion and erosion are phenomena that have significant impacts on coastal and estuarine ecosystems, infrastructure and socio-economic activities.

This process requires further studies, not only field observations, but also numerical modeling approaches. Numerical modeling to analyze the level of erosion and sedimentation that occurs in estuaries and beaches, as well as the relationship between accumulated discharge from rivers, tidal currents, and waves is one approach that can be taken in integrating the relationship between these factors to the resulting sedimentation and erosion into an alternative that can be used in this study. This model is certainly not only for the study of analyzing the level of erosion and sedimentation that occurs, but is expected to be an initial step to support further studies in the future both in predicting changes in estuary morphology and strategies in conducting good and accurate mitigation. In representing the model according to the conditions in the field, of course, the model carried out requires an accuracy test to approach the actual conditions.

Delft3D modeling is one of the numerical models that has been widely recognized and used by many researchers in conducting studies related to coastal engineering, especially in simulating hydrodynamic processes and changes in estuarine and coastal morphology [9,10,11,12,13,14]. The Delft3D numerical model

integrates the behavior of changing tidal currents, wave direction, sediment concentration and accumulated river discharge to simulate the dynamics of sediment transport and erosion patterns in the Manikin estuary and beach. Numerical models are very suitable in helping us to analyze, and estimate hydrodynamic cycles, erosion and sedimentation patterns, and sediment transport in an area at any given time [15].

Delft3D-Wave module as one of the modules used in the wave evolution model both in calculating propagation, generation by wind, and dissipation of wave energy [16]. Delft3D-Wave performs well in simulating waves as applied in Indonesian seas, such as in the sea of Banyuwangi and Bali in research to calibrate wave models with measurement data. [17]. In addition, Delft3D-Flow is also one of the other modules used in hydrodynamic simulations related to current phenomena and sediment transport by tides [18]. The use of Delft3D-Flow in sedimentation and erosion transport studies in Indonesia has also been widely used such as in sedimentation studies in the Ciletuh River Estuary, Sukabumi [19]. The Flow module is usually combined with the wave module in analyzing sediment transport that occurs in the estuary by considering the influence of river inflow, tides, and ocean waves. However, there are also many studies that only consider currents in sediment transport. As explained earlier, the use of Delft3D is very helpful in analyzing sedimentation, erosion, and morphological changes of estuaries and coastal areas.

RESEARCH SIGNIFICANCE

This research aims to model sedimentation and erosion that occurs in estuaries and beaches with the help of Delft3D application. The results of the study will be analyzed and aim to provide an overview of the level of erosion and sedimentation that occurs, identify erosion points within the study site domain boundaries and the influence of waves, tides, and discharge. In addition, testing the performance of the model created in representing the conditions that occur at the study research.

METHODOLOGY

This research has three objectives, the first is to analyze the level and points of sedimentation-erosion that occur based on visuals from the numerical model conducted. The second objective is to calibrate the model to assess its accuracy and performance. The third objective is to analyze the influence of waves, tidal currents, and river discharge in the sedimentation and erosion processes generated based on current with wave and current without wave model scenarios. In addition, this study also modeled erosion and sedimentation in the west and east seasons to see sedimentation and erosion patterns in different seasons.

A. RESEARCH LOCATION AND DATA COLECTION

The study site in this research is at the Manikin River Estuary, Kupang, East Nusa Tenggara.

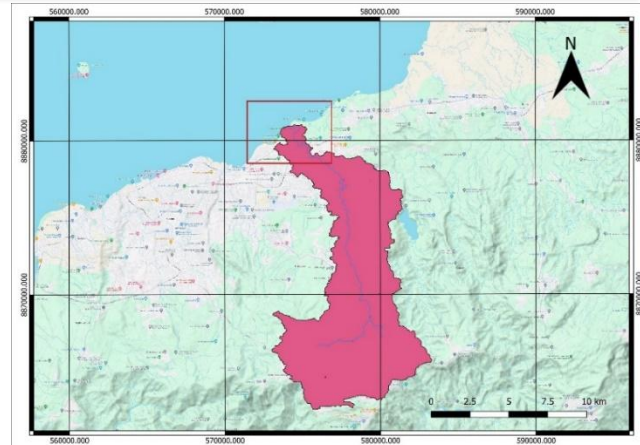


Figure 1 Research Location

This study used primary and secondary data. Primary data consisted of bed load (d_{50}), suspended load concentration (TSS), and topographic measurements of Manikin Estuary and Beach. Meanwhile, the secondary data used is the 2024 wave data sourced from ERA 5-Reanalysis European Centre for Medium-Range Weather Forecasts (ECMWF) with a resolution of 3.00 x 2.00 consisting of significant wave heights (Hs) per hour, peak period, wave direction, speed, wind direction and surface pressure [20]. In addition, bathymetric data was also used for the study location, and lidar data for the Manikin River obtained from the Geospatial Information Agency [21]. The discharge data used as input for the Delft3D model is the daily AWLR (Automatic Water Level Recorder) discharge data obtained from the Nusa Tenggara II River Basin Office (BWS NT-II). The tidal data used is tidal data from the Delft Dashboard June-December 2024, and tidal data from the BMKG Tenau Station obtained from SRGI BIG which will be used as calibration data with the Delft3D tidal model [22].

B. WAVE MODEL SET-UP

The wave model uses the Delft3D-Wave module in the Delft feature which uses SWAN waves which are the 3rd generation. SWAN waves in this study are very helpful in computing models on curved grids, plus coupling between Wave and Flow models. SWAN wave output from model computation can be in the form of one- and two-dimensional wave spectra [16].

Computation of the SWAN model in Delft3D using the equation [16,23] :

$$\frac{\partial}{\partial t} N + \frac{\partial}{\partial x} c_x N + \frac{\partial}{\partial y} c_y N + \frac{\partial}{\partial \sigma} c_\sigma N + \frac{\partial}{\partial \theta} c_\theta N = \frac{S}{\sigma} \quad (1)$$

The first term in the left-hand side of this equation represents the local rate of change of action density in time, the second and third term represent propagation of action in geographical space (with propagation velocities c_x and c_y in x - and y -space, respectively). The fourth term represents shifting of the relative frequency due to variations in depths and currents (with propagation velocity c_σ in σ -space). The fifth term represents depth-induced and current-induced refraction (with propagation velocity c_θ in

θ -space).. The term S ($= S(\sigma; \theta)$) at the right-hand side of the action balance equation is the source term in terms of energy density representing the effects of generation, dissipation and non linear wave-wave interactions [16].

Wave modeling processed by downscaling using 3 different grid levels. The wave data from ERA5-Reanalysis is used to generate wave height output at locations with smaller and finer scale grid levels. (level 3 grid in the estuary section).

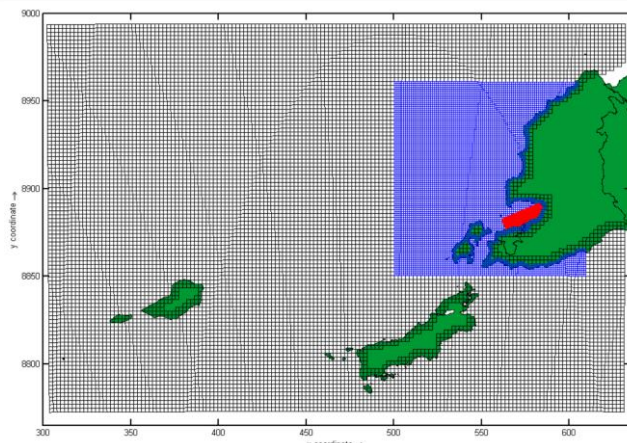


Figure 2 Downscaling Grid Model

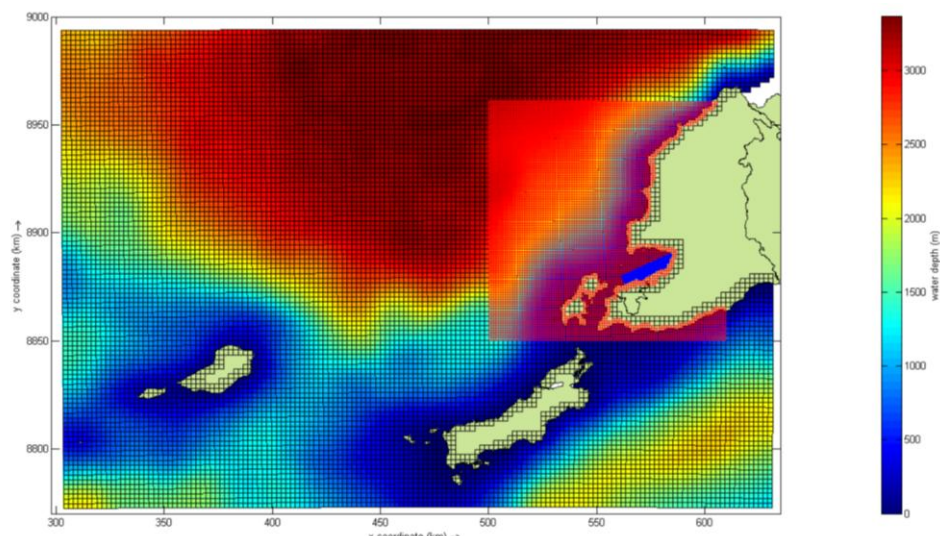


Figure 3 Bathymetri of Wave Model

Table 1 Describe of Grid Model

Grid	Size and Resolution	Boundary Condition	Description
Grid Level 1	$3.0^0 \times 2.0^0$ ($0.023^0 \times 0.023^0$)		ECMWF Wave Height and Wave Period in 2024
Grid Level 2	$1.0^0 \times 1.0^0$ ($0.01^0 \times 0.01^0$)	Wave Height and Period	Downscaling from Grid level 2
Grid Level 3	$0.2254^0 \times 0.0445^0$ ($0.00224^0 \times 0.00224^0$)		Downscaling from Grid level 3

C. FLOW MODEL SET-UP

The current model in this study uses the Delft3D-Flow feature which is used in the computation of tidal currents, and sediment transport in the Manikin estuary and coastal, and its morphological changes. This Delft3D-Flow model uses the depth-averaged continuity equation for an incompressible fluid [18]:

$$\nabla \cdot \mathbf{u} = 0 \quad (2)$$

With the kinematic boundary conditions at the water surface and seabed described as follows:

$$\frac{\partial \zeta}{\partial t} + \frac{1}{\sqrt{G_{\xi\xi}}\sqrt{G_{\eta\eta}}} \frac{\partial((d+\zeta)U\sqrt{G_{\eta\eta}})}{\partial \xi} + \frac{1}{\sqrt{G_{\xi\xi}}\sqrt{G_{\eta\eta}}} \frac{\partial((d+\zeta)V\sqrt{G_{\xi\xi}})}{\partial \eta} = (d + \zeta)Q \quad (3)$$

U and V are the average velocity with to depth for the velocity vector \mathbf{u} , d is the depth below the reference point, ζ is the elevation of the free surface from the reference point. $\sqrt{G_{\xi\xi}}$ and $\sqrt{G_{\eta\eta}}$ is the correction to the curvilinear coordinates. Where ξ and η are spatial direction for the

curvilinear coordinate system. The momentum equations for the ξ and η directions are presented as follows:

$$\frac{\partial u}{\partial t} + \frac{u}{\sqrt{G_{\xi\xi}}} \frac{\partial u}{\partial \xi} + \frac{v}{\sqrt{G_{\eta\eta}}} \frac{\partial u}{\partial \eta} - \frac{v^2}{\sqrt{G_{\xi\xi}} \sqrt{G_{\eta\eta}}} \frac{\partial \sqrt{G_{\eta\eta}}}{\partial \xi} + \frac{uv}{\sqrt{G_{\xi\xi}} \sqrt{G_{\eta\eta}}} \frac{\partial \sqrt{G_{\xi\xi}}}{\partial \eta} - fv = -\frac{1}{\rho_0 \sqrt{G_{\xi\xi}}} P_\xi + F_\xi + M_\xi \quad (4)$$

and

$$\frac{\partial v}{\partial t} + \frac{u}{\sqrt{G_{\xi\xi}}} \frac{\partial v}{\partial \xi} + \frac{v}{\sqrt{G_{\eta\eta}}} \frac{\partial v}{\partial \eta} + \frac{uv}{\sqrt{G_{\xi\xi}} \sqrt{G_{\eta\eta}}} \frac{\partial \sqrt{G_{\eta\eta}}}{\partial \xi} + \frac{v^2}{\sqrt{G_{\xi\xi}} \sqrt{G_{\eta\eta}}} \frac{\partial \sqrt{G_{\xi\xi}}}{\partial \eta} - fu = -\frac{1}{\rho_0 \sqrt{G_{\eta\eta}}} P_\eta + F_\eta + M_\eta \quad (5)$$

With $P_{\xi,\eta}$ is the pressure gradient, $F_{\xi,\eta}$ is the force due to Reynold's stress and $M_{\xi,\eta}$ is the contribution of external forces (wave, source and sink).

This study uses the Delft3D-Flow feature to compute the current wave model in sediment transport by coupling with Delft3D-Wave based on ERA5-Reanalysis wave height data [16,21].

The basic sediment transport equation for non-cohesive sediments uses the following equation:

$$q_b = 0.015 \rho_s u h \left(\frac{d_{50}}{h} \right)^{1.2} \left(\frac{u_e - u_{cr}}{[(s-1)gd_{50}]^{0.5}} \right)^{1.5} \quad (6)$$

Where ρ_s = sediment density, d_{50} = median of grain diameter, u = average velocity, h = water depth, u_e = average velocity with wave influence, u_{cr} = critical velocity of sediment grains, s = specific gravity of sediment grains and g = acceleration of gravity. Suspended sediment is calculated at the reference point with the Van Rijn equation (1984) as follows :

$$c_a = 0.015 \frac{d_{50}}{a} \frac{T^{1.5}}{D_*^{0.3}} \quad (7)$$

Where is c_a = sediment concentration at reference point a with maximum value 0.05, $D_* = d_{50}[(s-1)g/v^2]^{1/3}$, v = water viscosity and T = bed shear stress parameter. Erosion and deposition of suspended load are calculated based on the following equations:

$$D = w_s c_a \quad (8)$$

and

$$E = \varepsilon_s \frac{\partial c}{\partial z} \quad (9)$$

Dimana D = deposition flux, w_s = sediment fall velocity, E = erosion flux, ε_s = coefficient of sediment diffusion dan $\frac{\partial c}{\partial z}$ = sediment concentration gradient with depth calculated based on rouse profile.

Cohesive sediments were calculated based on the equation of Partheniades-Krone (1965):

$$E = M \left(\frac{\tau_{cw}}{\tau_{cr}} - 1 \right); \tau_{cw} > \tau_{cr} \quad (10)$$

$$D = w_s c_b \left(1 - \frac{\tau_{cw}}{\tau_{cr}} \right); \tau_{cw} < \tau_{cr} \quad (11)$$

Where E and D = flux of erosion and deposition of cohesive sediment, M = sediment erosion parameter, τ_{cw} = shear stress due to currents and waves, w_s = fall velocity of sediment particles and c_b = bed load concentration. Morphological changes were calculated based on sediment balance (Exner equation) for each sediment fraction:

$$\frac{\partial z}{\partial t} = \nabla \cdot \vec{q}_b - E + D \quad (13)$$

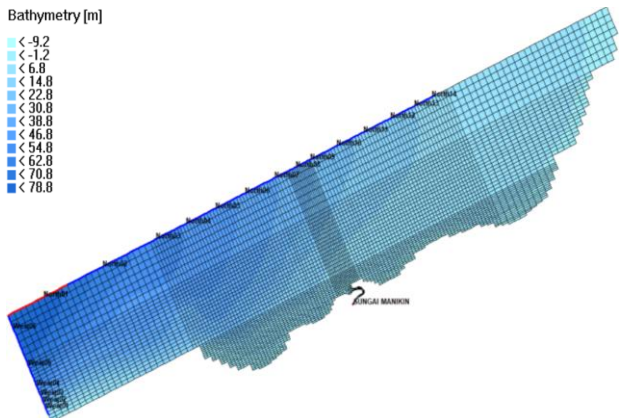


Figure 4 Boundary Condition of Flow Model

Table 2 Tidal Components Model

Tidal Component	Amplitude (m)	Phase (deg)	Formzahl Numbers
M2	0.7766	75.1751	
S2	0.4013	123.5049	
N2	0.1363	56.3114	
K2	0.1100	124.5936	
K1	0.2715	175.6801	
O1	0.1672	164.5927	
P1	0.0847	171.6652	0.3724
Q1	0.0392	158.0827	
MF	0.0126	8.9566	
MM	0.0067	8.7930	
M4	0.0039	309.2091	
MS4	0.0095	51.4821	
MN4	0.0023	344.0642	

The value of the tidal component is obtained from the Delft Dashboard and then the determination of the tidal type based on the Formzahl number of 0.37 ($0.25 < F < 1.5$) indicates that the type of tide that occurs at the study site is Mix Tide Prevailing Semi Diurnal.

D. MODEL CALIBRATION

1. Hydrodynamics Calibration

This study calibrates hydrodynamics for tides from DELFT3D modeling with tides recorded by BMKG Tenau Kupang to test the accuracy of the model. calibration carried out on August 12 - August 23, 2024

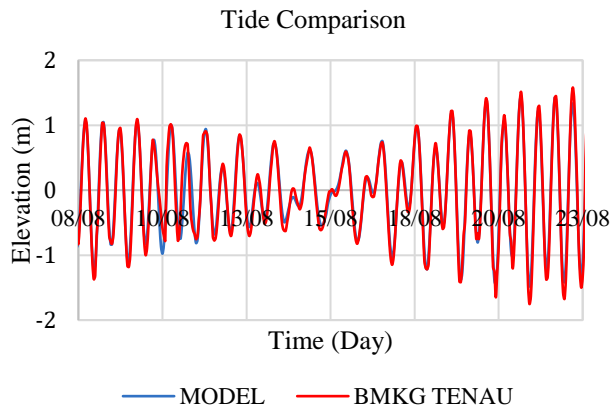


Figure 5 Calibration Tide

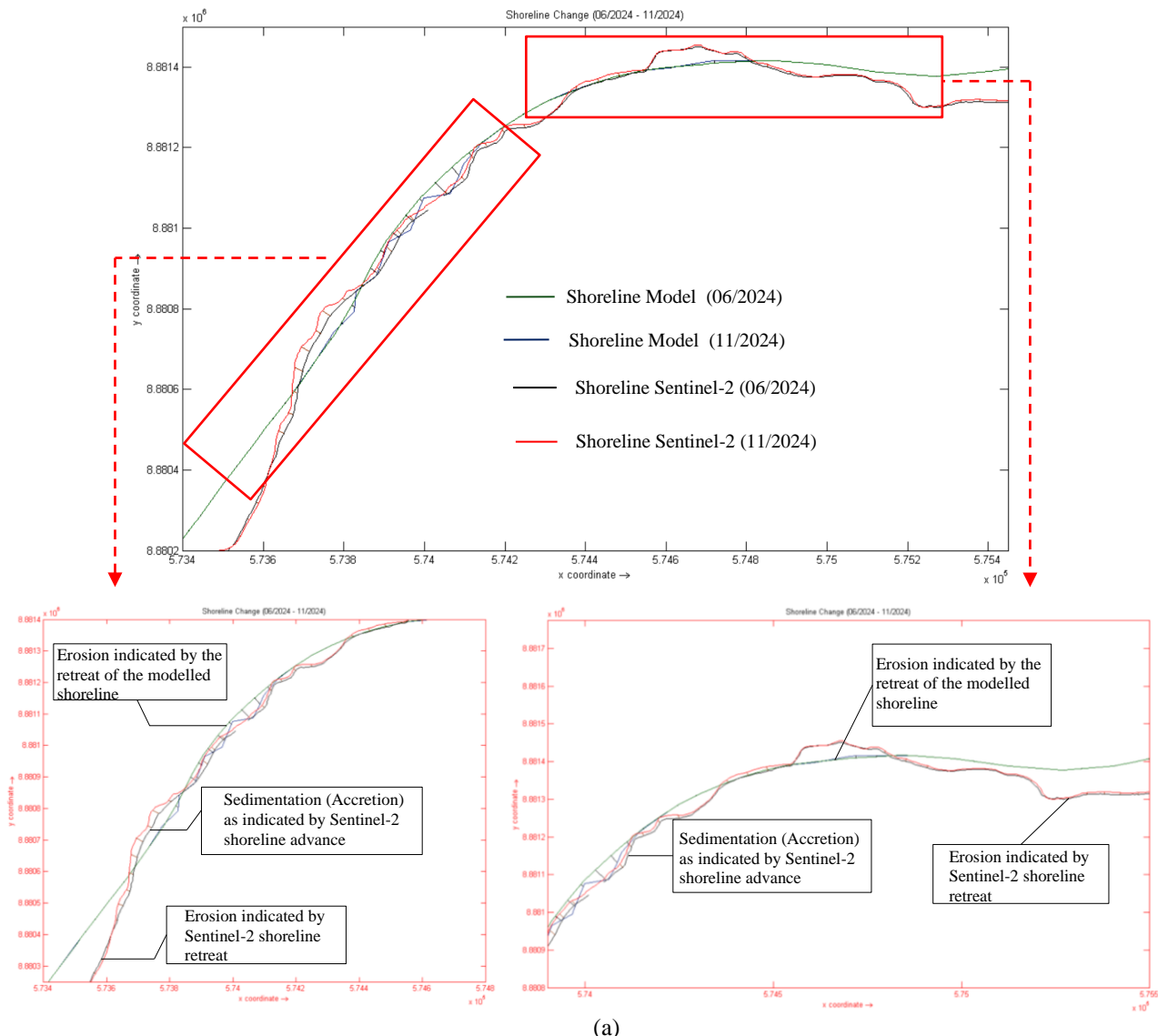
Table 3. Calibration of tide

Calibration	Tide model	Category
NSE	0.887	Good
RMSE	0.203	Good enough
MAPE	1.212	Very Good

The Delft3d modeled tides showed good criteria for NSE calibration, good enough for RMSE calibration, and very good for MAPE calibration. This indicates good validation of the model in interpreting the conditions occurring at the study site.

2. Shoreline Calibration

In addition to the tidal calibration, a qualitative calibration was also conducted by comparing the delft3d model shoreline to see the continuous pattern of change against shoreline changes from Sentinel-2 and Landsat-9 images. In this research, Sentinel satellite images were obtained by Copernicus [24], while Landsat-9 was obtained from USGS [25]. In addition, it also uses the help of CoastSat in generating the coastline. This is an alternative in testing the accuracy of the model due to data limitations, where there is no measurement data on morphological changes in estuaries and coastal in the concept of time series or with different times as a reference for calibrating morphological changes.



(a)

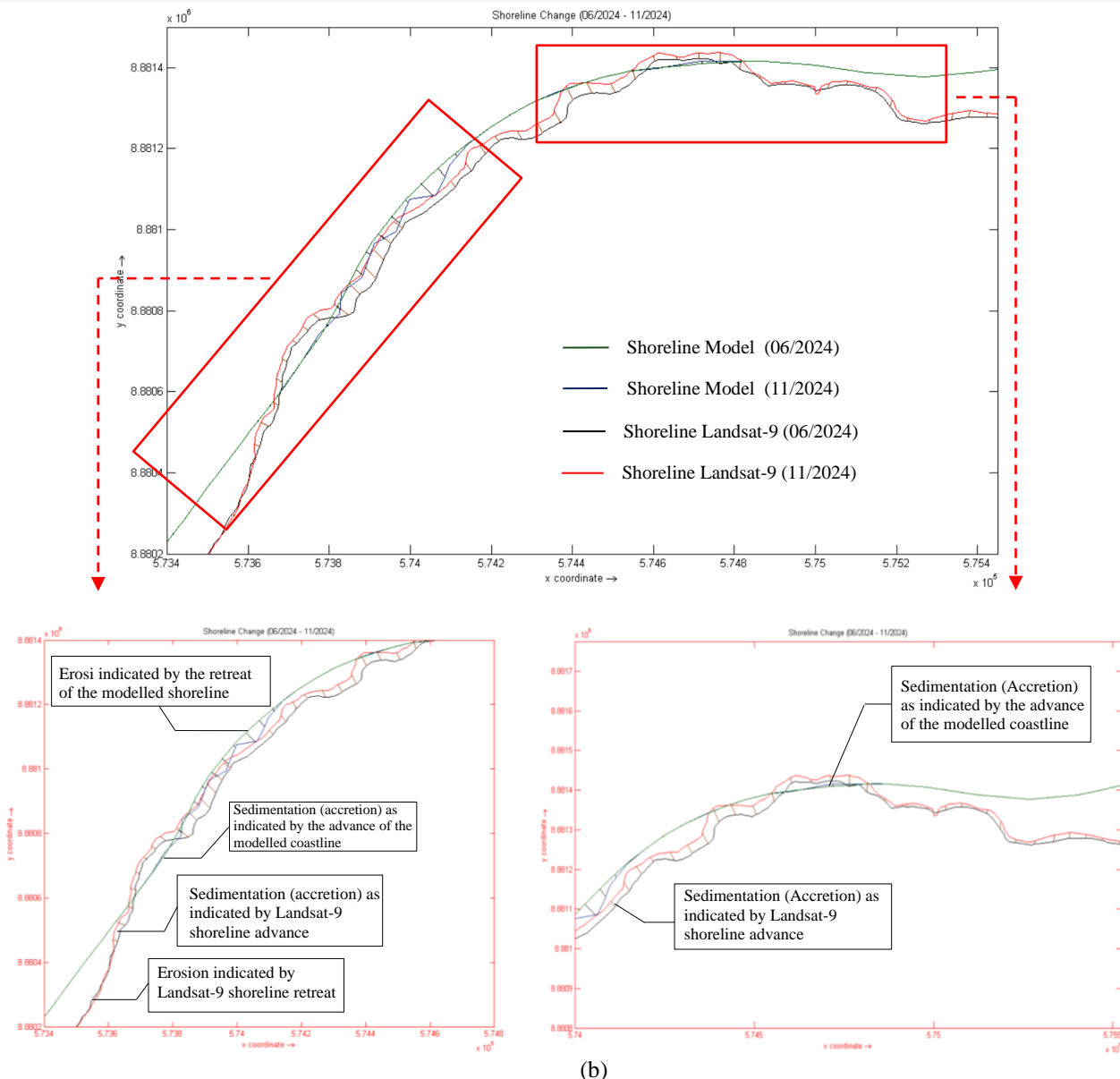


Figure 6. (a) Comparison of Delft3D Model Shoreline with Sentinel-2 Shoreline, (b) Comparison of Delft3D Model Shoreline with Landsat-9 Shoreline

Figure 6(a) shows the results of qualitative calibration between Delft3D modeling shoreline changes and actual Sentinel-2 satellite image data. The comparison of shoreline changes was carried out at two different times, from June to November 2024, where the time chosen adjusted to the time of availability of mind data with good Sentinel-2 resolution and avoided noise such as cloud cover, etc. Comparisons were made at critical locations that experienced significant shoreline changes. Based on the results of the qualitative comparison, it shows that the model is able to show the suitability of spatial shoreline change patterns. In addition, the selection of the modeled elevation 0 contour, which is the Delft3D coastline, shows the positional conformity of the modeled coastline to the sentinel-2 image coastline. However, there are still significant local differences from the modeled coastline when compared to the image data. Similar to the comparison with the Sentinel-2 image, Figure 6(b) shows

the qualitative calibration of the Delft3D model coastline with the Landsat-9 image. The model shows a pattern that is quite consistent with the Landsat-9 image data, although there are still differences between the model and the image coastline. Qualitatively, the Delft3D model is able to map the general trend of shoreline change, although the visuals of the model's shoreline tend to be smoother, showing more linear shoreline changes compared to Sentinel-2 and Landsat-9, which show more complex changes. This is due to the spatial accuracy, and readings of the imagery that tend towards short wave dynamics, as well as tidal change patterns. The author only explains the changes in the manikin coastline based on the delft3d model, where there was an average accretion of 1.10 m and an average erosion of 6.21 m during the modeling period from June to November 2024. These changes were averaged based on each coastline change transect point.

RESULTS AND DISCUSSIONS

A. WAVE CHARACTERISTICS

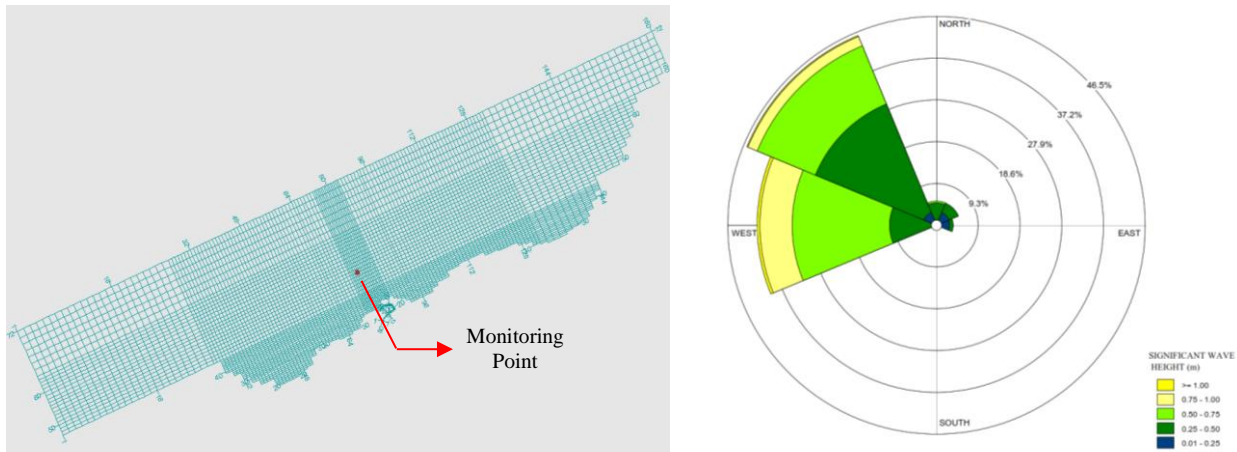
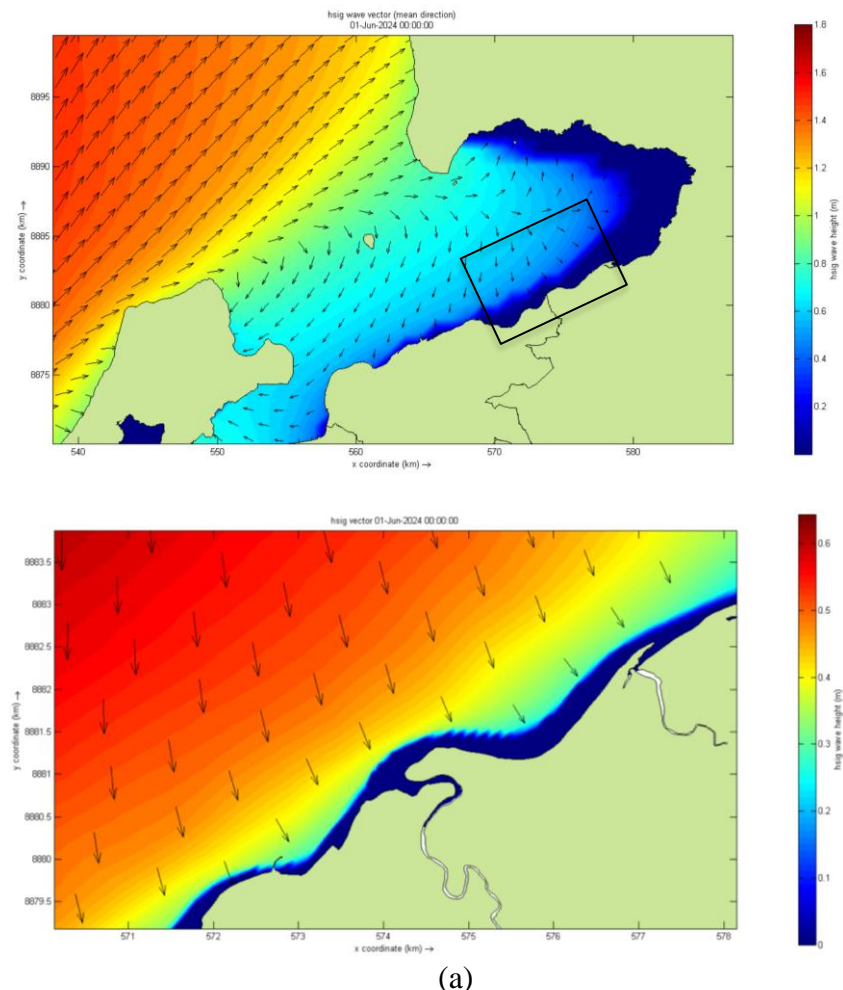


Figure 7. wave roses at the study research (estuary grid/ level 3 grid)

Figure 7 above is a wave rose showing the wave height for the incident direction of the Delft3D-Wave model in the simulated estuary grid area according to the Delft3D-Flow simulation time. For the boundary conditions (Figure 7), the dominant waves are from the southwest to northwest with wave heights of 0.00 - 1.80 m, while the waves are from the south with heights of 0.00 - 1.60 m. The wave

boundary conditions are downscaled to show the wave heights from the south. This wave boundary condition was downscaled to describe the wave scale through grid nesting at three different grid levels to draw more specific wave heights at the study site in the finest grid domain (estuary grid/ level 3).



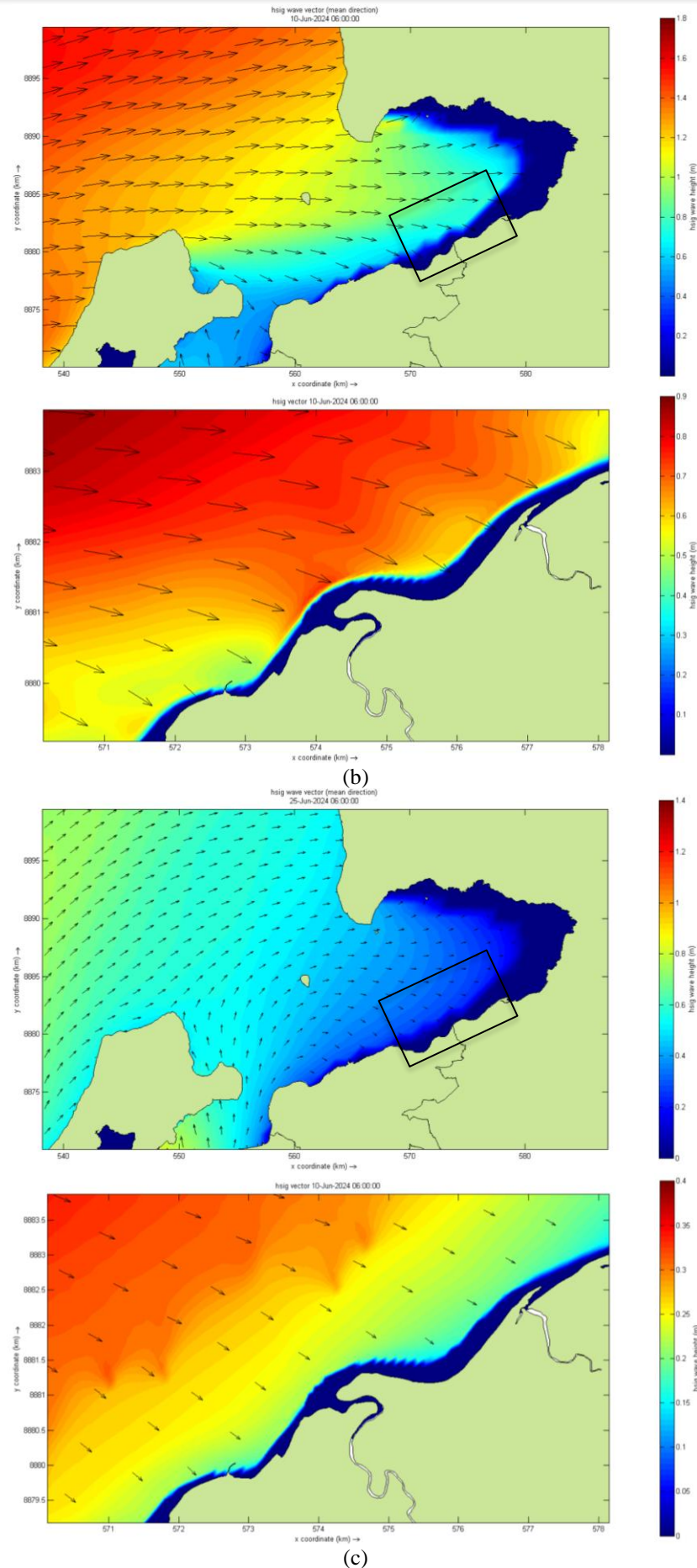


Figure 8. (a) Wave Direction from Southwest, (b) Wave Direction from West, (c) Wave Direction from South

Based on the modelling, the wave height in the study area tends to be low compared to high seas with wave heights ranging from 0.00 - 1.50 m. Figure 8 shows the characteristics of calmer waves and smaller energy the

closer to shallow water. The small wave height towards the shallower seabed shows the influence of shallow sea water on wave energy and height.

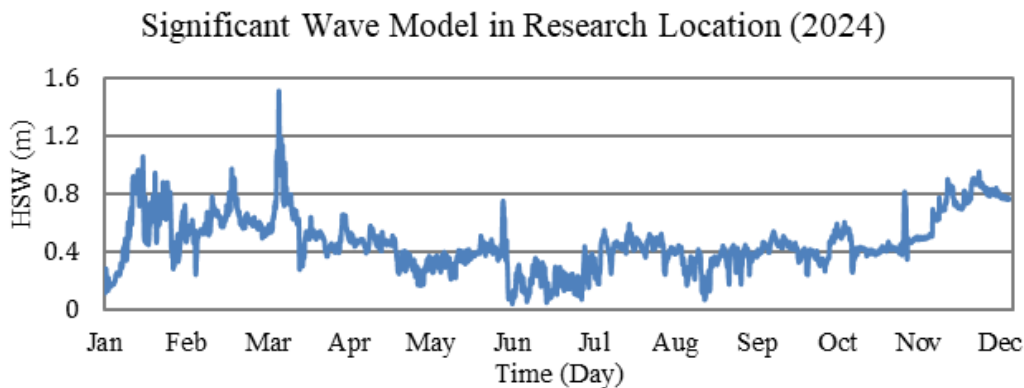


Figure 9. Significant Wave Height at Grid Level 3 Estuary

B. TIDE AND FLOW CHARACTERISTICS

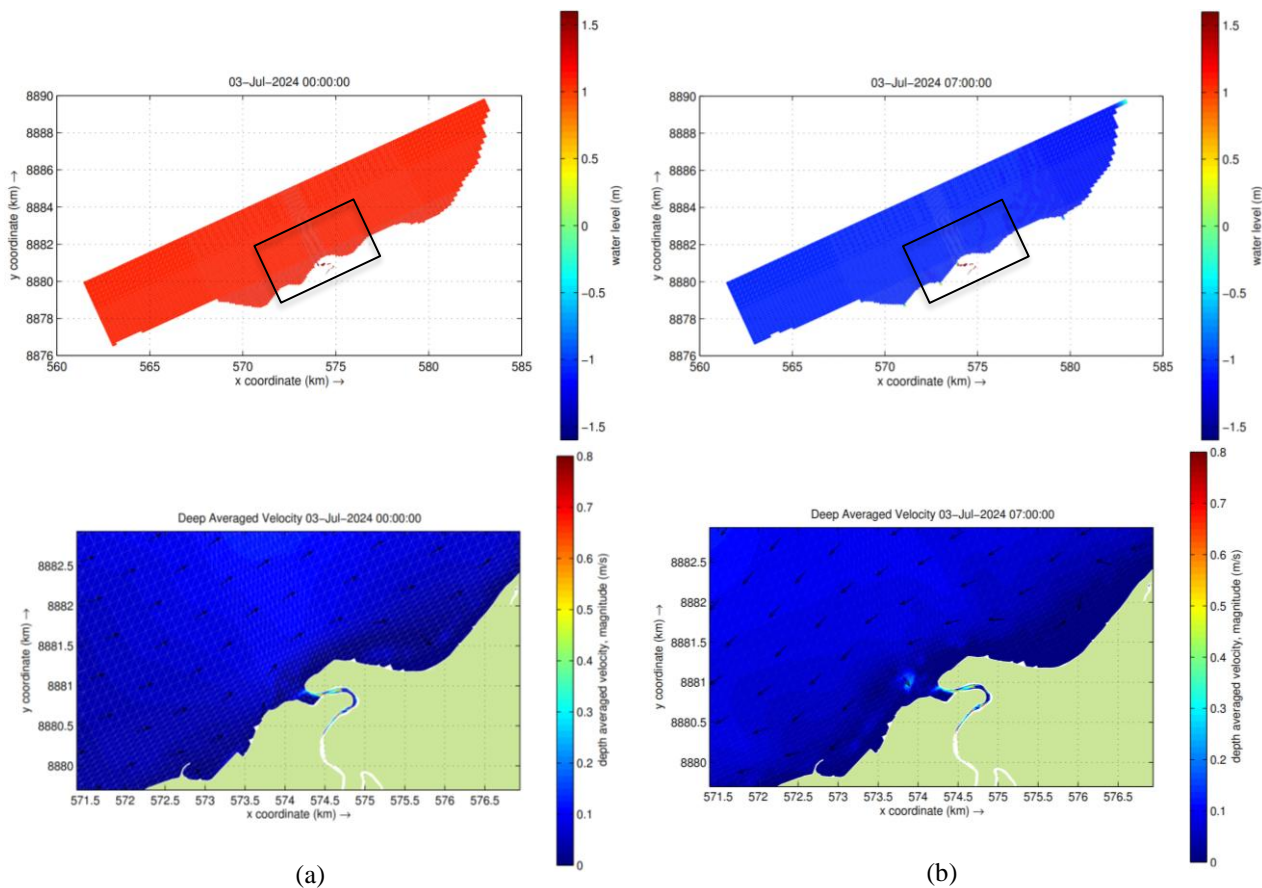


Figure 10. (a) Current Conditions at High Tide, (b) Current Conditions at Low Tide.

Figure 10 shows the modeling results, illustrating the relationship between the direction and fluctuations in current velocity based on the tidal patterns that occur and the back-and-forth movement of the currents. In Manikin seas, during the transition from high tide to low tide, the current velocity decreases until it reaches a turning point. When the tide begins to rise, the current increases again towards the estuary and river, reaching its maximum at the

peak of the tide, then weakening again as it turns to low tide. In the river channel, the current velocity during low tide is relatively high because the flow moves from the river to the sea. Conversely, at high tide, the current speed is smaller due to the convergence of the incoming sea flow with the river discharge. The current speed in the waters around the estuary ranges from 0.01 to 0.16 m/s with a tidal range of 1.50 m and -1.50 m. The current velocity in

the upstream area from the estuary to the mouth of the estuary is around 0.10–0.80 m/s. This shows that the current velocity tends to be smaller the closer it is to the seabed, which indicates the influence of shallow seawater on current velocity fluctuations.

C. EROSION / SEDIMENTATION AND MORPHOLOGY CHANGES

Erosion/sedimentation modeling was conducted on June 1 - December 2, 2024 based on the sampling time of

bed load and suspended load concentrations, as well as topographic measurements of the Manikin Estuary and Coastal in August 2024.

Simulation shows that in the upstream area of the estuary there is erosion of 0.00 - 0.40 m and sedimentation of 0.00 - 0.30 m. Erosion and sedimentation are more concentrated in the estuary area and around the coast. The erosion that occurs is 0.0-0.60 m and sedimentation is 0.0 - 0.70 m.

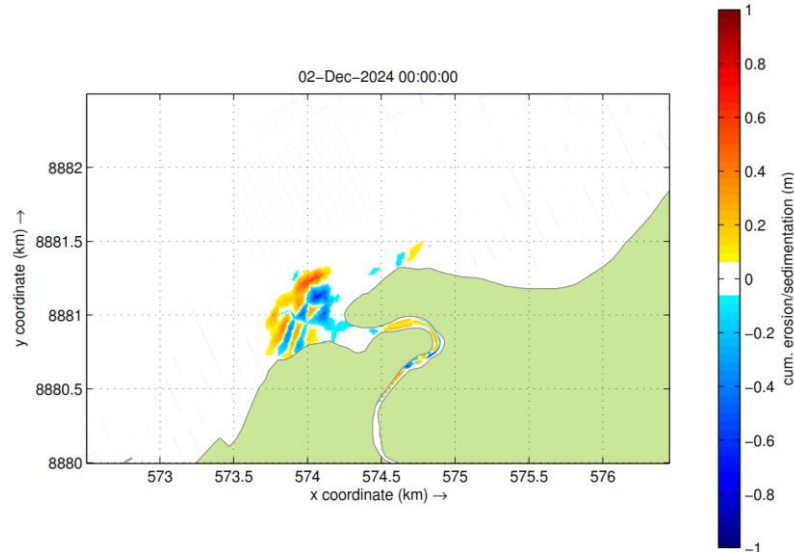


Figure 11. Estuary and Coastal Erosion/ Sedimentation Modeling Results

The condition of the estuary along the winding coast causes sediment carried by the current to accumulate more at the mouth of the estuary. In addition, the direction of incoming

waves that are not perpendicular to the position of the beach affects the sediment transport process that occurs at the study location.

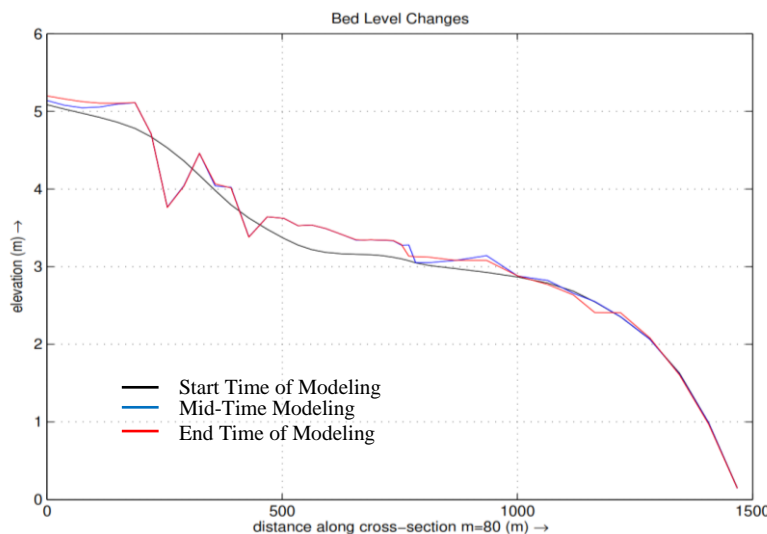


Figure 12. Estuary and Beach Bottom Changes

D. THE INFLUENCE OF WAVES AND CURRENTS ON EROSION/SEDIMENTATION IN ESTUARIES AND COASTAL

The effect of waves and currents on sedimentation and erosion in this study was analyzed with a model

scenario in the form of modelling without waves (Delft3D-Flow) which was compared with the results of the Delft3D Flow-Waves 01 June – 02 December 2024 previous results in figure 10.

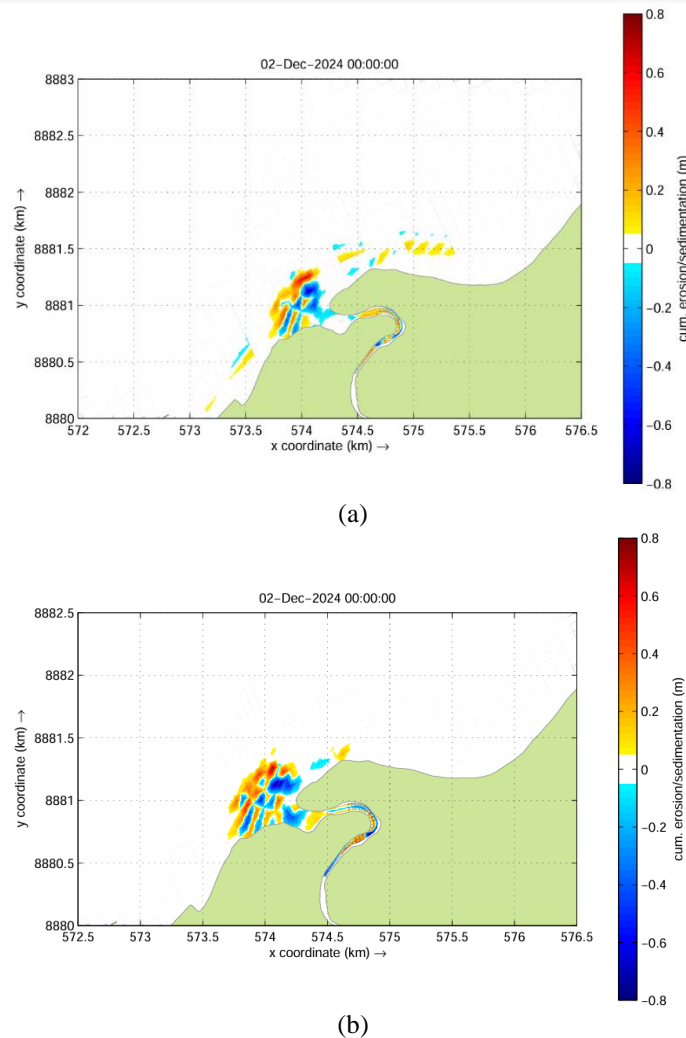


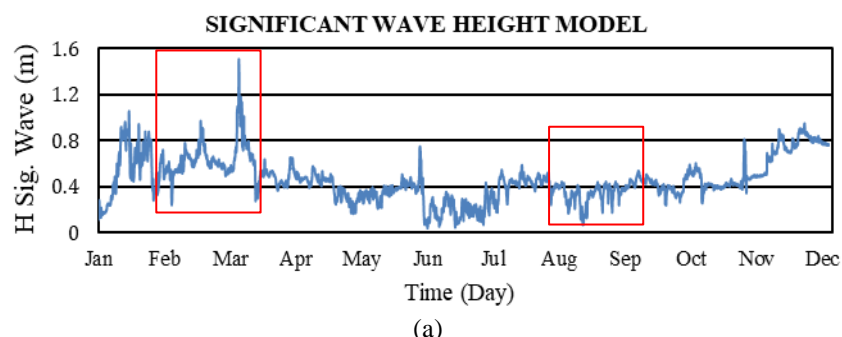
Figure 13 (a) Delft3D Flow + Wave Erosion/Sedimentation Model, (b) Delft3D Flow Erosion/Sedimentation Model

Based on erosion and sedimentation modeling scenarios focused on estuaries and coastal areas in analyzing the influence of waves, tides, and river discharge on sediment transport processes, the results show that:

1. The coupling simulation of Delft3D-Flow and Delft3D Wave results in a wider and more even sediment distribution process, and the resulting accretion-erosion pattern is more complex. The presence of wave influence enlarges sediment transport in the estuary and beach area, thereby reducing sediment deposition in the estuary due to wave influence which causes sediment transport to be more widespread along the coastline..

2. The Delft3D Flow simulation without considering the influence of waves shows morphological changes that are more concentrated around the river mouth. It can be observed that sediment distribution is more limited, driven only by tidal effects and river discharge accumulation. As a result, changes occurring in the upstream and estuary areas are more significant compared to Scenario 1. The higher levels of erosion and sedimentation in the upstream area, caused by river currents, are directly proportional to the erosion and sedimentation in the estuary and coastal areas, due to the absence of wave energy influence in the sediment transport process.

E. EROSION AND SEDIMENTATION MODELING IN WET AND DRY SEASONS



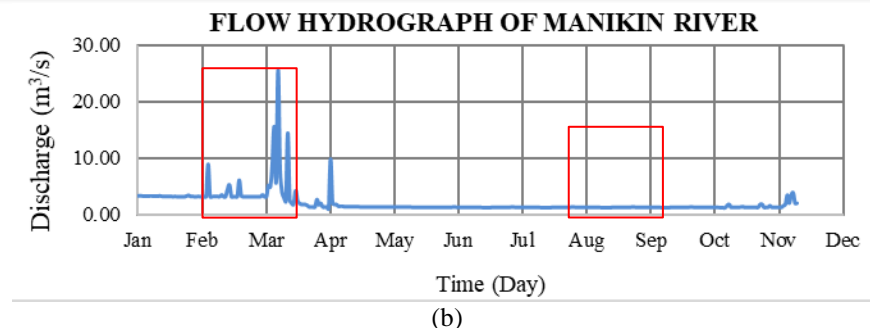


Figure 14 (a) Time Series of Significant Wave Height on western season and eastern season, (b) Time series of Manikin River flow discharge on west season and east season

Sedimentation and erosion models were conducted in the west (wet) and east (dry) seasons with a modeling time duration of 1 month for each season. This modeling aims to determine the characteristics of sedimentation and erosion that occur in different seasons, and also to see the level of erosion-sedimentation that occurs in both seasons. This erosion-sedimentation model adapts to the wave

characteristics (Delft3D-Wave) which are reviewed based on the dominant wave conditions that occur during the wet season based on the influence of the west monsoon, and the dominant waves that occur during the dry season by the influence of the east monsoon. Meanwhile, the flow model (Delft3D-Flow) follows the wave conditions by considering the Manikin river discharge data.

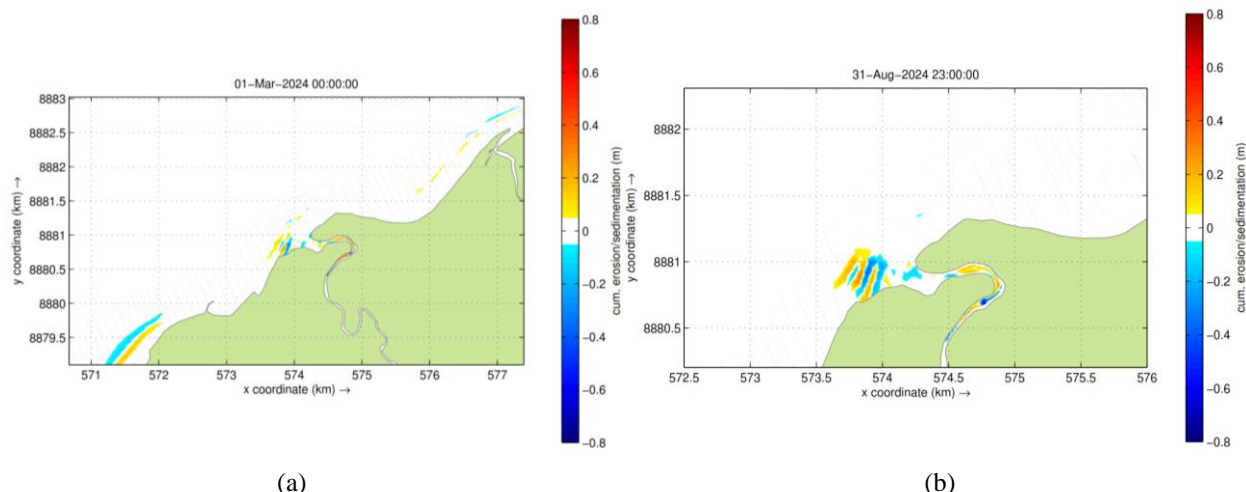


Figure 15 (a) Erosion and Sedimentation on West Season, (b) Erosion and Sedimentation on East Season

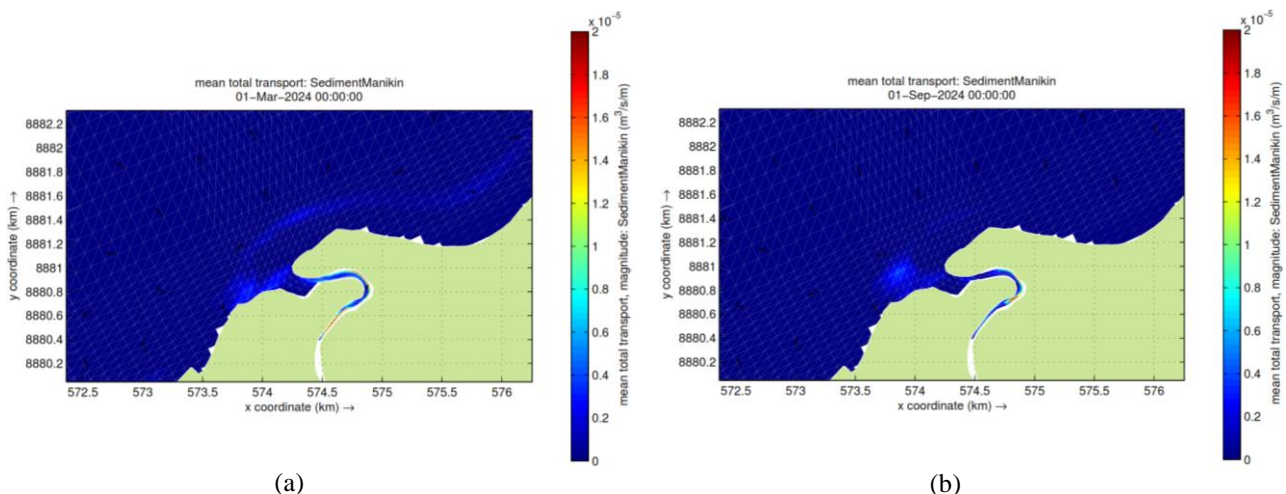


Figure 16 (a) Total Transport of Sediment on West Season, (b) Total Transport of Sediment Erosion and Sedimentation on East Season.

The figure shows that during the wet season (west season), erosion and sedimentation are quite high compared to the dry season (east season). The high waves around the

estuary and the large discharge during the wet season are very influential in sediment transport. Sedimentation and erosion along the coast are generally more influenced by

high waves in the wet season. The erosion trend varies, with the beach being 0.10 - 0.60 m thick. Erosion occurs not only in the estuary and Manikin beach, but also in the northeast and southwest of Manikin Beach. The sedimentation varies from 0.10 - 0.50 m. Similar to erosion, sedimentation generated in the model also occurred in the northeast and southwest of the study site. Erosion and sedimentation trends that occur in the wet season are generally influenced by relatively high waves for coastal areas and flood discharge during the rainy season which causes high erosion and sedimentation in river sections. The small discharge and relatively low waves during the dry season show smaller sedimentation and erosion compared to the wet season. The total sediment transport in the wet season modeling period ranges from 0.00001 to 0.6550 kg/s/m (after conversion with density). Figure 14 (b) shows sedimentation and erosion occurring in the estuary and beach, indicating that the event was more influenced by ocean waves even though the dry season wave height was smaller than the wet season. Erosion is 0.10 - 0.30 m thick and sedimentation is 0.10 - 0.30 m thick. Sedimentation and erosion that tend to occur in the estuary area are also caused by the winding coastal conditions, so that sediments carried by currents along the coast accumulate at the mouth of the estuary, and at the same time these conditions are also subject to scouring by currents along the coast. The total sediment transport in the dry season modeling ranged from 0.00001 to 0.39620 kg/s/m (after conversion with density). This was influenced by the small river sediment supply, so that the sediment transport supply process was more dominated by wave and tidal factors.

CONCLUSIONS

Research aimed at modeling erosion and sedimentation in estuaries and manikin beaches using the Delft3D application shows varying trends. Based on the results and discussion, it can be concluded that the model indicates more accumulated erosion and sedimentation in the estuary and coastal areas, as the outflow of river sediment supply, alongshore currents, and wave action. These factors contribute to dominant sedimentation and erosion processes in the estuary and coastal zones. The model shows changes in the coastline during the modeling period from June to November 2024, where the average erosion and accretion on the coastline is 6.21 m and 1.10 m. The model output in the form of tidal predictions shows good calibration in representing the conditions at the study site, with NSE value of 0.887, RMSE of 0.203, and MAPE indicating an error rate of 1.212.

The scenarios developed to analyze the influence of waves and currents (tides and river discharge) indicate that the current model without considering wave influence results in erosion and sedimentation that are more concentrated around the estuary, due to limited sediment distribution driven only by tidal currents and river discharge. In the current and wave model scenario, wave energy enhances sediment transport, preventing accumulation around the estuary and causing the sediment transport to spread more widely beyond the estuarine area.

Erosion and sedimentation that occur during the wet season are influenced by the high waves of the west monsoon which are dominant to sedimentation and erosion on the beach, and large flood discharge during the rainy season so that erosion and sedimentation in the river are quite large with a thickness of 0.10 - 0.60 m for erosion and 0.10 - 0.50 m for sedimentation. The dry season shows erosion and sedimentation that is more influenced by the east monsoon sea waves, although it is lower than the wave height during the wet season. Erosion that occurs during the dry season has a thickness of 0.10 - 0.30 m, and sedimentation that occurs has a thickness of 0.10 - 0.30 m.

ACKNOWLEDGMENTS

The authors gratefully acknowledge Balai Wilayah Sungai Nusa Tenggara II (BWS NT-II) for providing automatic water level data used as input data for the Manikin River. The authors also acknowledge the European Centre for Medium-Range Weather Forecasts (ECMWF) for providing ERA5 data used in wave modeling, the Geospatial Information Agency (BIG) for providing bathymetry and tidal data for the study site, and colleagues who have assisted in this research.

REFERENCES

- [1] B. Triadmodjo, *Teknik Pantai*. Yogyakarta: BETA, 1999.
- [2] P. I. D. Putri and M. S. B. Kusuma, "Kondisi Hidrodinamika dan Transpor Sedimen di Perairan Muara Sungai Ayung dengan Simulasi Delft 3D," *J. Apl. Tek. Sipil*, vol. 21, no. 4, pp. 385–396, 2023 <http://iptek.its.ac.id/index.php/jats>
- [3] M. Elliott and A. K. Whittfield, "Challenging paradigms in estuarine ecology and management," *Estuar. Coast. Shelf Sci.*, vol. 94, no. 4, pp. 306–314, 2011, doi: 10.1016/j.ecss.2011.06.016.
- [4] M. W. Brand, L. Guo, E. D. Stein, and B. F. Sanders, "Multi-decadal simulation of estuarine sedimentation under sea level rise with a response-surface surrogate model," *Adv. Water Resour.*, vol. 150, January, p. 103876, 2021, doi: 10.1016/j.advwatres.2021.103876.
- [5] L. C. Van Rijn, "Unified View of Sediment Transport by Currents and Waves . I: Initiation of Motion, Bed Roughness, and Bed-Load Transport," *J. Hydraul. Eng.*, June, pp. 649–667, 2007.
- [6] N. Yuwono, *Perencanaan Bangunan Jetty, Laboratorium Hidraulika dan Hidrologi*. Yogyakarta: Universitas Gadjah Mada, 1994.
- [7] L. X. Tu, "Hydrodynamics, sediment transport at estuaries and coastal zone of the Mekong delta Modelling for Mekong delta," March, 2017.
- [8] H. Elmilady, "3D Sediment Dynamics in an Estuarine Strait. MSc Thesis. UNESCO-IHE, Delft, The Netherlands," March, 2016.
- [9] G. R. Lesser, J. A. Roelvink, J. A. T. M. van Kester, and G. S. Stelling, "Development and validation of a three-dimensional morphological model," *Coast. Eng.*, vol. 51, no. 8–9, pp. 883–915,

Oct. 2004,
doi: 10.1016/J.COASTALENG.2004.07.014.

[10] L. Brakenhoff, R. Schrijvershof, J. van der Werf, B. Grasmeijer, G. Ruessink, and M. van der Vegt, “From ripples to large-scale sand transport: The effects of bedform-related roughness on hydrodynamics and sediment transport patterns in delft3d,” *J. Mar. Sci. Eng.*, vol. 8, no. 11, pp. 1–25, 2020, doi: 10.3390/jmse8110892.

[11] J. Wang, A. Chu, Z. Dai, and J. Nienhuis, “Delft3D model-based estuarine suspended sediment budget with morphodynamic changes of the channel-shoal complex in a mega fluvial-tidal delta,” *Eng. Appl. Comput. Fluid Mech.*, vol. 18, no. 1, 2024, doi: 10.1080/19942060.2023.2300763.

[12] N. G. Plant *et al.*, “Journal of Geophysical Research : Earth Surface,” pp. 300–316, 2014, doi: 10.1002/2013JF002871.Received.

[13] H. Elmilady, M. van der Wegen, D. Roelvink, and B. E. Jaffe, “Intertidal Area Disappears Under Sea Level Rise: 250 Years of Morphodynamic Modeling in San Pablo Bay, California,” *J. Geophys. Res. Earth Surf.*, vol. 124, no. 1, pp. 38–59, 2019, doi: 10.1029/2018JF004857.

[14] X. Zhang, S. Fagherazzi, N. Leonardi, and J. Li, “A Positive Feedback Between Sediment Deposition and Tidal Prism May Affect the Morphodynamic Evolution of Tidal Deltas,” *J. Geophys. Res. Earth Surf.*, vol. 123, no. 11, pp. 2767–2783, 2018, doi: 10.1029/2018JF004639.

[15] A. H. Fattah, Suntoyo, H. A. Damerianne, and Wahyudi, “Hydrodynamic and Sediment Transport Modelling of Suralaya Coastal Area, Cilegon, Indonesia,” *IOP Conf. Ser. Earth Environ. Sci.*, vol. 135, no. 1, 2018, doi: 10.1088/1755-1315/135/1/012024.

[16] Deltares, “Delft3D-WAVE Simulation of of Short-Crested With SWAN User Manual,” Netherland: Deltares, 2024.

[17] I. D. B. JBS, S. Damarnegara, A. Dastgheib, and J. Reynolds, “Significant Wave Height Model Calibration in The Sea Around Banyuwangi and Bali,” *J. Civ. Eng.*, vol. 39, no. 1, p. 76, 2024, doi: 10.12962/j20861206.v39i1.20395.

[18] Deltares, “Delft3D-FLOW Simulation of Multi-Dimensional Hydrodynamics Flows and Transport Phenomena, Including Sediments User Manual,” Netherland: Deltares, 2024.

[19] Y. Suryadi *et al.*, “Kajian Sedimentasi di Muara Sungai ciletuh, Kabupaten Sukabumi,” *J. Tek. Sipil*, vol. 27, no. 2, p. 147, 2020, doi: 10.5614/jts.2020.27.2.5.

[20] “European Centre for Medium-Range Weather Forecasts (ECMWF) Reanalysis 5-th Generation.” <https://cds.climate.copernicus.eu/datasets/reanalysis-5-single-levels>

[21] Badan Informasi Geospasial, ‘Batimetri Nasional.’ <https://tanahair.indonesia.go.id/demnas/#/batnas>

[22] “Sistem Referensi Geospasial Indonesia.” <https://srgi.big.go.id/>

[23] G. Whitham, *Linear and Nonlinear Waves*. New York: John Wiley & Sons (Wiley-Interscience), 1974.
<https://dataspace.copernicus.eu/explore-data/data-collections/sentinel-data/sentinel-2>
 “United State Geological Survey (USGS).” <https://explorer.usgs.gov>